Pergamon

Bioorganic & Medicinal Chemistry Letters, Vol. 7, No. 22, pp. 2825-2830, 1997

0960-894X/97 $17.00 + 0.00

PII: S0960-894X(97)10098-1

USE OF CoMFA IN VALIDATING THE CONFORMATION USED IN DESIGNING 4-(1*H*-BENZIMIDAZOLE-2-CARBONYL)PIPERIDINES WITH H_1/NK_1 RECEPTOR ANTAGONIST ACTIVITY

Roy J. Vaz,* George D. Maynard, Elizabeth M. Kudlacz, Larry D. Bratton, John M. Kane, Scott A. Shatzer, and Robert W. Knippenberg

Hoechst Marion Roussel, Inc., 2110 E. Galbraith Road, Cincinnati, Ohio 45215

Abstract: Support for the conformation used in the design of a series of 4-(1*H*-benzimidazole-2-carbonyl)piperidines with dual histamine H_1/tachykinin NK_1 receptor antagonist activity has been presented. Comparative Molecular Field Analysis(CoMFA) for both receptor binding affinites of the series as well as overlays with several crystal structures of selective receptor antagonists support the conformation.

The design rationale for the dual histamine H_1 and tachykinin NK_1 receptor antagonists described in the earlier publication[1] centered around designed 3-arylpyrrolidine dual NK_1 and NK_2 receptor antagonists[2] and the histamine receptor antagonist MDL 28,163[3] (Figure 1), Compound **38** (Table 1) (H_1 IC_{50} = 59 nM[4]). The design of the 3-arylpyrrolidine dual NK_1 and NK_2 receptor antagonists,[2] included constraints on SR 48,968[5] to design MDL 103,220 and then overlays of the low energy conformations of MDL 103,220 with those of CP 96,345[6] to design MDL 105,212 (Figure 1). Combining the benzimidazole substructure from MDL 28,163 with the N-(3,4,5-trimethoxybenzamido)-3-aryl pyrrolidine substructure from MDL 105,212 lead to the design of dual H_1/NK_1 antagonists such as **2**, MDL 103,896, and the analogs in Table 1. The compounds in Table 1 were used in the construction of Comparative Molecular Field Analyses (CoMFA)[7] for both histamine H_1 and tachykinin NK_1 receptor affinity.

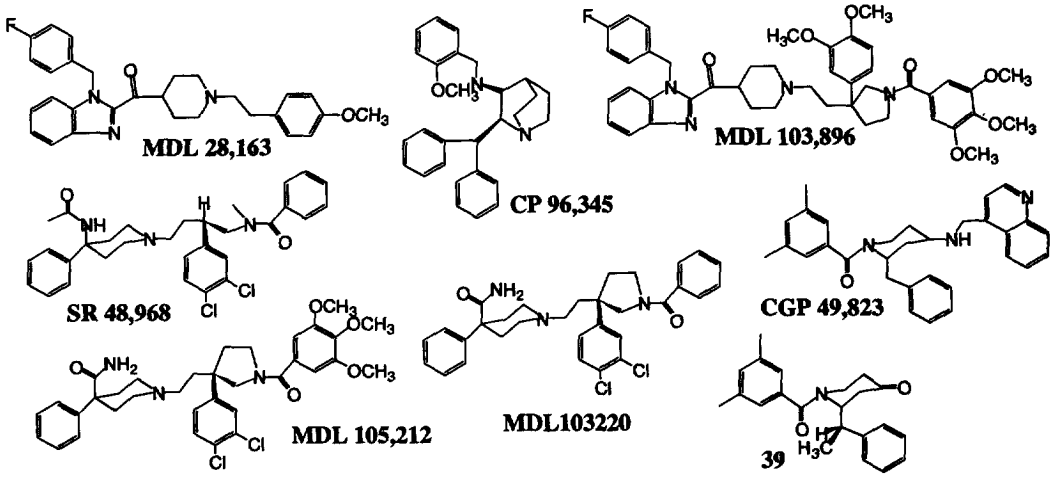

Figure 1: MDL 28,163, SR 48,968, CGP 49,823 and other molecules from earlier work.

Table 1: Structures used together with activities both measured and fitted from the CoMFA using alignment A in Figure 2a.

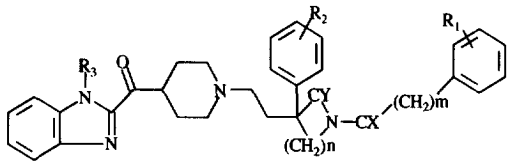

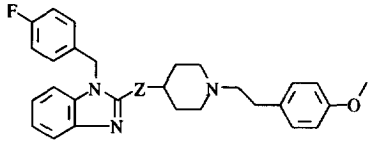

Compd	X	Y	n	m	R1	R2	R3	Z	pNK1	pH1	pNK1(fit)	pH1(fit)
1	O	H_2	2	0	3,4,5-$(OEt)_3$	3,4,-$(OMe)_2$	4-F-$PhCH_2$		5.91	6.80	6.37	6.77
2	O	H_2	2	0	3,4,5-$(OMe)_3$	3,4,-$(OMe)_2$	4-F-$PhCH_2$		7.36	6.48	6.92	6.38
3	O	H_2	2	0	3,4,5-$(OMe)_3$	3,4,-Cl_2	morpholinoethyl		7.82	6.26	7.68	6.32
4	O	H_2	2	0	3,4,5-$(OMe)_3$	3,4,-Cl_2	2-PyridylCH_2		7.50	6.36	7.44	6.41
5	O	H_2	2	0	3,4,5-$(OMe)_3$	3,4,-Cl_2	4-F-$PhCH_2$		7.47	6.55	7.28	6.45
6	O	H_2	3	0	3,4,5-$(OMe)_3$	3,4,-Cl_2	4-F-$PhCH_2$		6.54	6.67	6.52	6.79
7	O	H_2	2	0	3,4,5-$(OMe)_3$	2,4-F_2	4-F-$PhCH_2$		6.52	6.36	7.19	6.46
8	H_2	O	2	0	3,4,5-$(OMe)_3$	4-F	$CH_3CH_2OCH_2CH_2$		6.93	6.60	6.92	6.64
9	O	H_2	2	1	3-$OCH(CH_3)_2$	3,4-OCH_2O	4-F-$PhCH_2$		6.54	6.60	6.27	6.58
10	O	H_2	2	0	3,4,5-$(OMe)_3$	3,4,-Cl_2	$CH_3CH_2OCH_2CH_2$		7.51	6.47	7.61	6.31
11	O	H_2	2	0	3,4,5-$(OMe)_3$	-	4-F-$PhCH_2$		7.47	6.63	7.31	6.46
12	O	H_2	2	0	3,4,5-$(OMe)_3$	-	-		7.44	6.30	7.32	6.31
13	O	H_2	2	0	3,4,5-$(OMe)_3$	-	2-PyridylCH_2		7.56	6.44	7.56	6.39
14	O	H_2	2	0	3,4,5-$(OMe)_3$	3,4,-$(OMe)_2$	-		6.98	5.71	7.08	5.96
15	O	H_2	2	0	3,4,5-$(OMe)_3$	3,4,-Cl_2	-		7.27	6.39	7.22	6.29
16	O	H_2	2	0	3,4,5-$(OMe)_3$	3,4-OCH_2O	4-F-$PhCH_2$		6.84	6.69	6.89	6.58
17	O	H_2	2	0	3,4,5-$(OMe)_3$	4-CF_3	4-F-$PhCH_2$		6.93	6.33	7.12	6.44
18	O	H_2	2	0	3,4,5-$(OMe)_3$	-	4-CH_3O_2C-$PhCH_2$		7.65	5.93	7.98	5.94
19	O	H_2	2	0	-	3,4,-$(OMe)_2$	4-F-$PhCH_2$		6.21	6.62	5.75	6.67
20	O	H_2	2	0	2,4-Cl_2	3,4-OCH_2O	4-F-$PhCH_2$		5.00	6.89	5.40	6.85
21	O	H_2	2	0	3,4,5-$(OMe)_3$	3,4,-Cl_2	$HO_2C(CH_2)_3$		7.76	5.00	7.70	5.02
22	O	H_2	2	0	2,3,4-$(OMe)_3$	3,4-OCH_2O	4-F-$PhCH_2$		6.43	6.59	6.31	6.60
23	O	H_2	2	0	3,4,5-$(OMe)_3$	-	$CH_3CH_2OCH_2CH_2$		7.59	6.42	7.61	6.41
24	O	H_2	2	0	3,4,5-$(OMe)_3$	-	2-$HO_2CPhO(CH_2)_3$		7.57	5.04	7.37	5.13
25	O	H_2	2	0	3,4,5-$(OMe)_3$	-	2-$CH_3O_2CPhO(CH_2)_3$		7.81	6.00	7.74	6.00
26	O	H_2	2	0	3,4,5-$(OMe)_3$	-	2-Furanyl$CH_2OCH_2CH_2$		7.93	6.35	7.92	6.24
27	O	H_2	2	0	3,4,5-$(OMe)_3$	4-OMe	2-PyridylCH_2		7.37	6.30	7.52	6.30
28	O	H_2	2	0	3,4,5-$(OMe)_3$	4-F	2-PyridylCH_2		7.66	6.25	7.47	6.39
29	O	H_2	2	0	3,4,5-$(OMe)_3$	3,4,-$(OMe)_2$	$CH_3CH_2OCH_2CH_2$		7.39	6.20	7.34	6.28
30	O	H_2	2	0	3,4,5-$(OMe)_3$	3,4,-$(OMe)_2$	4-CH_3O_2C-$PhCH_2$		7.63	6.02	7.61	5.87
31	O	H_2	2	0	3,4,5-$(OMe)_3$	3,4,-Cl_2	$CH_3CH_2O_2C(CH_2)_3$		7.57	6.02	7.53	6.12
32	O	H_2	2	0	3,4,5-$(OMe)_3$	-	2-FuranylCH_2		7.68	6.53	7.71	6.47
33	O	H_2	2	0	3,4,5-$(OMe)_3$	-	3-PyridylCH_2		7.57	6.38	7.56	6.41
34	O	H_2	2	0	3,4,5-$(OMe)_3$	-	4-HO_2CPhCH_2		7.45	4.47	7.57	4.47
35	O	H_2	2	0	3,4,5-$(OMe)_3$	3,4,-$(OMe)_2$	4-HO_2CPhCH_2		7.00	4.56	7.14	4.47
36	O	H_2	2	0	3,4,5-$(OMe)_3$	-	4-PyridylCH_2		7.43	6.55	7.36	6.53
37								-N=	5.86	7.33	5.75	7.35
38								-(C=O)-	5.28	7.23	5.40	7.23

The structures shown in Table 1 were constructed in the two conformations (two alignments) shown in Figure 2 and were subjected to a 3D-QSAR, CoMFA. Conformation A was derived by conformational searching to locate low energy overlay conformations between the 3-arylpyrrolidines, CP 96,345 and various other NK_1 selective receptor ligands[2]. Conformation B was selected solely on the basis of low relative energy. In Table 1, only compounds **5** and **28** were optically pure. However, all the other compounds were constructed such that the chiral center was *R*. Compounds **4**, **13**, **27**, **28**, and **33** have either a 2- or 3-picolyl group. For each CoMFA alignment, two conformations for each of the these compounds were constructed with the pyridyl nitrogen pointing either outwards with respect to the rest of the molecule or inwards (shielded). Then for each alignment, analyses for both H_1 receptor affinity and NK_1 receptor affinity were done, with the conformation of these compounds having the pyridyl nitrogen on the same side. In both alignmentA and B, the conformation with the pyridyl nitrogen exposed, produces the more statistically significant CoMFA. A similar set of analyses was performed for both H_1 and NK_1 activities with the morpholino nitrogen as a free base and in a protonated state in compound **3**. Both analyses with the free base were more statistically significant.

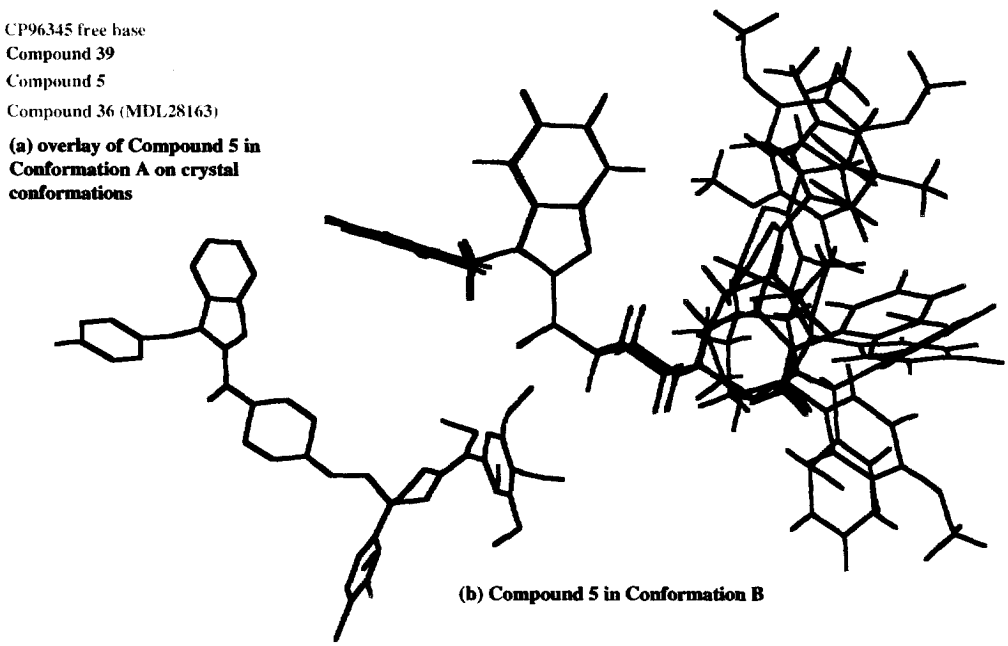

Figure 2: Compound 5 in the two comformations that were evaluated. (a) Conformation A has various crystal structures of selective antagonists overlaid. (b) Conformation B which had worse statistical significance in CoMFA then Conformation A

The statistical analysis of the CoMFA's obtained from these two alignments (with the pyridyl nitrogens exposed for the compounds **4**, **13**, **27**, **28**, and **33** and the morpholino nitrogen in the free base form in compound **3**) are in Table 2. Besides providing a more statistically significant correlation with cross-validation, alignment A, is supported by two other pieces of information. The first is the overall overlap with the crystal structure of compound **38**, MDL 28,163.[8] The second is the overlap with the crystal structure of the free base form of CP 96,345 (Cambrdige Crystallographic Database Ref. Code YAFJOE).[9] Also, recent[10] crystallographic data[11] on one of the chiral intermediates, compound **39** (Figure 1), involved in the synthesis of conformationally restricted analogs of NK_1 antagonist CGP 49,823 (Figure 1), also allowed a nice overlay with the alignment A (Figure 2a). This overlay shows **5**, and the crystal structure of compound **39**. The key to this overlay is the excellent overlap provided by the two benzene rings of CP 96,345, those of compound **39** and those in **5**, the overlay of the lone pair of the hydrogen bond acceptors (the oxygen of the carbonyl group in compound **5** the secondary amine in CP 96,345 and the oxygen of the amide carbonyl in compound **39** as shown in magenta, as well as the tertiary amine of CP 96,345, the position in compound **39** corresponding to the tertiary amine of CGP 48,923 and the piperidine nitrogen in cpd **5**. These were the same groups used in overlapping molecules for all the CoMFA work done.

Table 2: PLS results from the CoMFA performed on the H1 and NK1 antagonist activities using the two alignments shown in Figures 2a and 2b. The regions used had a 1A grid spacing.

	component 1	component 2	component 3	component 4	component 5
NK_1 alignment A					
Standard Error of Prediction	0.512	0.481	0.48	0.471	0.492
q_squared	0.495	0.568	0.582	0.609	0.587
Standard Error of Estimate	0.444	0.37	0.287	0.23	
r_squared	0.621	0.744	0.851	0.907	
contribution: steric				0.674	
electrostatic				0.326	
H_1 alignment A					
Standard Error of Prediction	0.297	0.25	0.232	0.232	0.227
q_squared	0.773	0.843	0.868	0.873	0.881
Standard Error of Estimate	0.246	0.178	0.142	0.111	0.094
r_squared	0.844	0.92	0.951	0.971	0.98
contribution: steric					0.476
electrostatic					0.524
NK_1 alignment B					
Standard Error of Prediction	0.511	0.502	0.498	0.495	0.512
q_squared	0.497	0.529	0.55	0.568	0.552
Standard Error of Estimate	0.441	0.382	0.293	0.218	
r_squared	0.625	0.727	0.844	0.916	
H_1 alignment B					
Standard Error of Prediction	0.401	0.37	0.377	0.418	0.453
q_squared	0.586	0.657	0.654	0.586	0.529
Standard Error of Estimate	0.325	0.273			
r_squared	0.727	0.813			

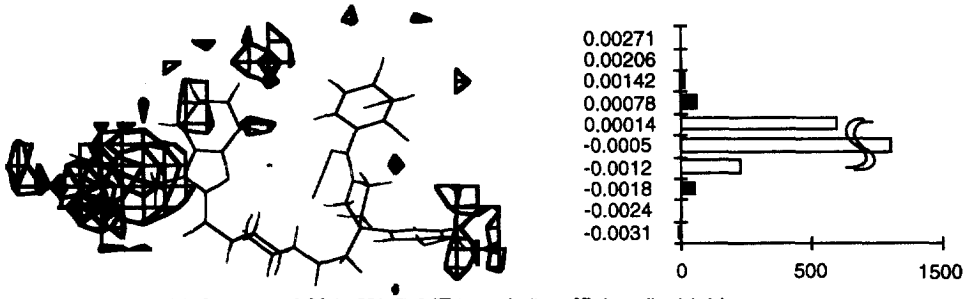

(a) Compound **20** in H1 CoMFA steric "coefficients" with histogram

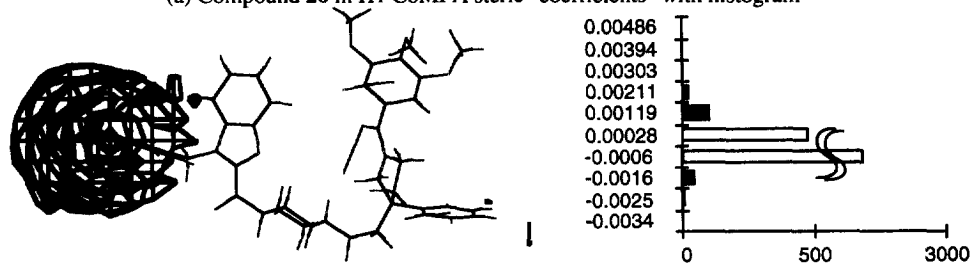

(b) Compound **34** in H1 CoMFA electrostatic "coefficients" with histogram

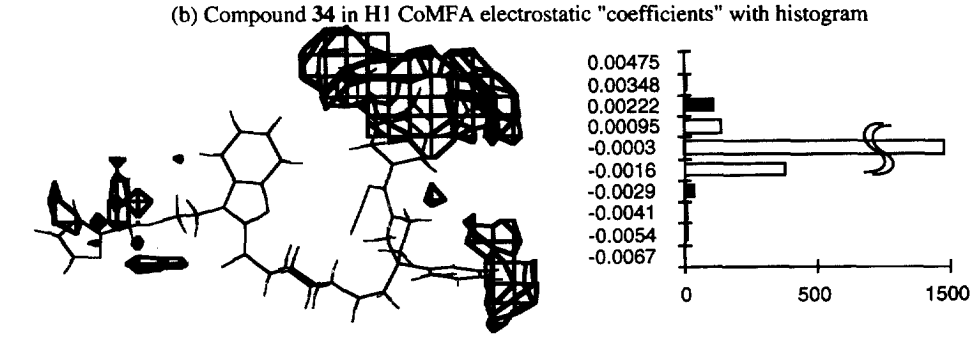

(c) Compound **26** in NK1 CoMFA steric "coefficients" with histogram

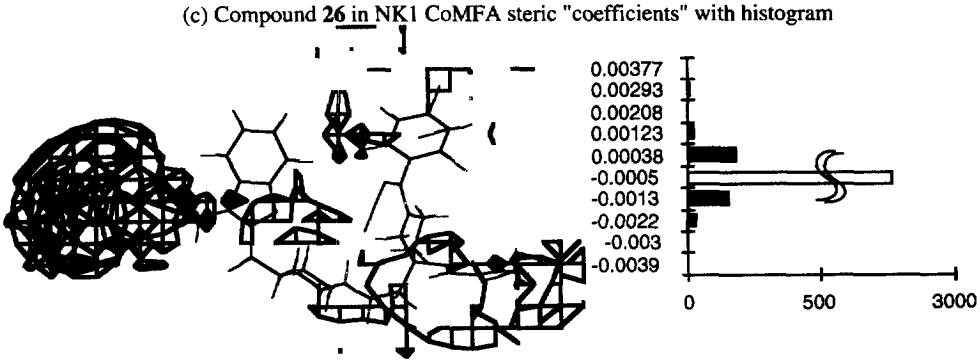

(d) Compound **20** in NK1 CoMFA electrostatic "coefficients" with histogram

Figure 3: (Coefficient)*(Standard Deviation) or "coefficient" plots with active compounds shown in the steric "coefficient" plots and less active compounds in the electrostatic "coefficient" plots.

The CoMFA standard deviation times QSAR coefficient" plots, also called the coefficient plots in the text here for both the steric as well as the electrostatic fields for the NK_1 as well as the H_1 3D-QSAR's are shown in Figure 3. Figure 3a shows one of the most active H_1 antagonists in the dual antagonist series in the H_1 steric coefficient plot with the fluorobenzyl group occupying the positive contour region where steric substitution enhances antagonist activity. Figure 3b shows one of the least active H_1 antagonists in the dual antagonist series in the H_1 electrostatic coefficient plot with the carboxyl group occupying the coefficient region that supports positively charged groups. Figure 3c shows one of the most active NK_1 antagonists in the dual antagonist series in the NK_1 steric coefficient plot with the tri methoxy substituted phenyl ring of the benzamide group occupying a positive contour region. Figure 3d shows one of the least active NK_1 antagonists in the dual antagonist series in the NK_1 electrostatic coefficient plot.

An overall observation made on the two sets of coefficient plots is that the benzamide end of the molecules in Table 1 seem to harbor NK_1 antagonist activity without significantly affecting H_1 antagonist activity. The benzimidazole end of the structures (the other end) affects H_1 antagonist activity without adversely affecting NK_1 antagonist activity. This could account for a single molecule with functionality at different ends having dual antagonist activity against different receptors without necessarily adopting two low energy conformations. Again, the overlap of compound **5** with the three structures having selective antagonist activity against H_1 and NK_1 activity respectively with very little in common between the two (Figure 2a) supports this observation.

Conclusion

Support of the conformation used to design dual antagonists of the H_1 and NK_1 receptors has been provided using statistical (3D-QSAR CoMFA) validation as well as overlap with selective H_1 and NK_1 receptor antagonists with little in common between them.

References and Notes

1. Maynard, G. D.; Bratton, L. D.; Kane, J. M.; Burkholder, T. P.; Santiago, B.; Stewart, K. T.; Kudlacz, E. M.; Shatzer, S. A.; Knippenberg, R. W.; Farrell, A. M.; Logan, D. E. *Bioorg. Med. Chem. Lett.* **1997**, *accompanying paper.*
2. Burkholder, T. P.; Kudlacz, E. M.; Le, T. B.; Knippenberg, R. W.; Shatzer, S. A.; Maynard, G. D.; Webster, M. E.; Horgan, S. W. *Bioorg. Med. Chem. Lett.* **1996**, *6*, 951.
3. Carr, A. A.; Hay, D. A.; Kane, J. M.; Staeger. M. A. *J. Org. Chem.* **1990**, *55*, 1399.
4. Kudlacz, E. M.; Shatzer, S. A.; Logan, D. E.; Olsen, K.; Knippenberg, R. W.; Hsieh, L.; Esteve, H.; Kehne, J.; Maynard, G. *Int. Arch. Allergy Immunol.* **1997**, *in press.*
5. (a) Emonds–Alt, X.; Vilain, P.; Goulaouic, P.; Proietto, V.; Van Broeck, D.; Advenier, C.; Naline, E.; Neliat, G.; Le Fur, G.; Breliere, J.-C. *Life Sci.* **1992**, *50*, PL101. (b) Emonds–Alt, X.; Proietto, V.; Van Broeck, D.; Advenier, C.; Naliat, G.; Le Fur, G.; Breliere, J.-C. *Bioorg. Med. Chem. Lett.* **1993**, *3*, 925.
6. (a) Lowe, J. A. III *Med. Res. Rev.* **1996**, *16*, 527. (b) McLean, S. *Med. Res. Rev.* **1996**, *16*, 297.
7. Cramer, R. D. III; Patterson, D. E.; Bunce, J. D. *J. Am. Chem. Soc.* **1988**, *110*, 5959.
8. X-ray analysis of MDL 28,163 was performed by Dr. J. C. Huffman (**1994**, Report No. 94703).
9. Lowe, J. A. III; Drozda, S. E.; Snider, R. M.; Longo, K. P.; Zorn, S. H.; Morrone, J.; Jackson, E. R.; McLean, S.; Bryce, D. K.; Bordner, J.; Nagahisa, A.; Kanai, Y.; Suga, O.; Tsuchiva, M. *J. Med. Chem.* **1992**, *35*, 2591.
10. (a) Veenstra, S. J.; Hauser, K.; Betschart, C. *Bioorg. Med. Chem. Lett.* **1997**, *7*, 347. (b) Veenstra, S. J.; Hauser, K.; Betschart, C. *Bioorg. Med. Chem. Lett.* **1997**, *7*, 351.
11. Thanks to S. J. Veenstra who provided the crystallographic information for compound **10** in ref 10a.

(*Received in USA* 15 *August* 1997; *accepted* 25 *September* 1997)